

Original Research Paper

Glenoid shape is sexually dimorphic: A geometric morphometric analysis and supplement to the Walch classification system

Matthew J. Zdilla, D.C.^{1,2,3*}; Evan D. French, M.A., D.P.T.^{1,4}; Halee N. Sowinski¹, Uriel Alfaro-Gomez⁵; Santos Guzmán-López, M.D., Ph.D.⁵; Rodrigo Elizondo-Omaña, M.D., Ph.D.⁵; Alejandro Quiroga-Garza, M.D., M. Surg., Ph.D.⁵

1. Department of Pathology, Anatomy, and Laboratory Medicine (PALM), West Virginia University School of Medicine, Morgantown, WV, USA

2. Department of Biological Sciences, West Liberty University, West Liberty, WV, USA

3. Department of Graduate Health Sciences, West Liberty University, West Liberty, WV, USA

4. Division of Physical Therapy, School of Rehabilitation and Communication Sciences, Ohio University, Athens, OH, USA

5. Department of Human Anatomy, Universidad Autónoma de Nuevo León, Nuevo León, Mexico

Article history

Received: 12 January 2023

Revised: 23 January 2023

Accepted: 24 January 2023

*Corresponding Author: Dr. Matthew J. Zdilla, Department of Pathology, Anatomy, and Laboratory Medicine (PALM), West Virginia University School of Medicine, Robert C. Byrd Health Sciences Center, Morgantown, West Virginia, 26506 (USA)
Email: matthew.zdilla@hsc.wvu.edu

Abstract: Uniform assessment of the glenoid anatomy is fundamental in establishing uniform standards of care. Subjectivity in classification inherent in the absence of quantification permits deficiency in glenoid assessment methods (e.g., Walch classifications). Therefore, this report aims to objectively quantify the variance of glenoid fossa contours in both sexes via geometric morphometric techniques. A total of 135 glenoid fossae from 135 adult Mexican individuals, who had undergone CT scanning for non-shoulder-related reasons, were randomly selected for this study. Geometric morphometric analysis, including principal component analysis, canonical variate analysis, and two-block partial least squares analysis, was performed on glenoid contours in coronal and axial planes among males and females of varied age groups. The canonical variate analysis of the glenoid revealed sexual dimorphism in both the coronal and axial glenoid contours. Males tend to have a more concave glenoid contour than females, especially in the axial plane. Partial least squares analysis revealed a shape-relationship between coronal and axial contours—when coronal contours are relatively concave, axial contours also exhibit concavity; conversely, when there is minimal concavity in one dimension, there tends to be minimal concavity in the other. This manuscript establishes a novel means of assessing the glenoid cavity through geometric morphometrics; in doing so, the objective and quantifiable methods can be an important supplement to evolving glenoid assessments such as the Walch classification system. The novel approach used in this research revealed sexual dimorphism in the shape of the glenoid cavity as well as a relationship between coronal and axial contours.

Keywords: anatomy; arthroplasty; glenohumeral joint; scapula; shoulder; Walch classification

Introduction

Consideration of the geometric variance of the glenoid fossa is important for glenohumeral arthroplasty procedures. The Walch classification

and subsequent iterations of the Walch classification, categorize varied glenoid fossae based upon shape and the relationship with the humeral head as assessed through two-dimensional CT scans in the axial plane. Based upon morphologic features identified in the scans, glenoids are divided into

types and specific subtypes (Fig. 1) (Walch *et al.*, 1999). The categorization of glenoid shape variation has, hence, guided clinical decision making.

The varied contours of glenoid fossae and their relationship with the humeral head position, described by the Walch classification of primary glenohumeral osteoarthritis, provide insight to the pre-operative determination of surgical approach, the intra-operative technique, and the post-operative survival of a prosthesis (Walch *et al.*, 1999; Bouchaib *et al.*, 2014; Vo *et al.*, 2017). Regarding pre-operative decision making, identification of an advanced Type B2 biconcave glenoid may steer surgical decision making toward posterior augmented glenoid designs or even a reverse prosthesis (Denard and Walch 2013; Kersten *et al.*, 2015). Intra-operatively, when reaming a pathologically concave glenoid (Walch classification Type A), the convexity of the reamer should be optimally adapted to the curvature of the glenoid (Karelse *et al.*, 2015). Post-operatively, the morphologic features addressed by the Walch classification, may affect glenoid implant survivability (Walch *et al.*, 1999; Vo *et al.*, 2017). Asymmetric load distribution is inherent to varied glenoid – humeral head shapes and orientations; one glenoid-humeral head configuration may cause a so-called rocking-horse effect at the glenoid, which may occur vertically or horizontally, and loosen the glenoid component of the prosthesis (Franklin *et al.*, 1988; Walch *et al.* 1999; Matsen *et al.* 2008). The posterior subluxation of the humeral head seen in Type B joints may be responsible for glenoid loosening due to a horizontal rocking-horse effect (Walch *et al.*, 1998). On the other hand, Type A glenohumeral joints have been suggested to have adequate stability for a prosthesis due to symmetrical load distribution and absence of subluxation (Walch *et al.*, 1999).

The Walch classification and its subsequent modifications and iterations are imperfect. While most studies have identified excellent intraobserver reliability, these same studies have also identified only fair/moderate interobserver reliability (Scalise *et al.*, 2008; Nowak *et al.*, 2010; Kidder *et al.*, 2012; Bercik *et al.*, 2016; Lowe *et al.*, 2017; Vo *et al.* 2017). Deficiencies of glenoid assessment methods may be attributable to subjectivity in classification inherent in the absence of quantification. In other words, disagreement may exist in defining the difference between minor and major concavity (e.g., between an

A1 and A2 classifications). However, uniform assessment of the glenoid anatomy is important in establishing uniform standards of care. Therefore, this report aims to objectively quantify the variance of glenoid fossa contours via geometric morphometric techniques.

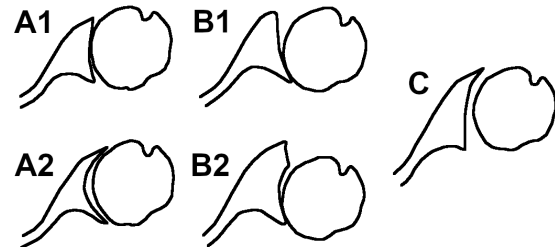


Figure 1. Line drawings representing the original Walch classifications (axial plane). Type A glenoids have central erosion that ranges from minor (A1) to major (A2). Type B glenoids have posterior wear associated with posterior humeral subluxation ranging from minor (B1) to major (B2), the latter possessing a biconcavity. Type C glenoids are dysplastic with $>25^\circ$ of retroversion with a humeral head that is centered upon the glenoid (C). Adapted from Karelse A, Leuridan S, Van Tongel A, Debeer P, Van Der Sloten J, Denis K, De Wilde LF. Consequences of reaming with flat and convex reamers for bone volume and surface area of the glenoid; a basic science study.

J Orthop Surg Res. 2015. **10**:181

(<http://creativecommons.org/licenses/by/4.0/>)

Materials and Methods

The research was approved by the Ethics and Research Committees of the Universidad Autónoma de Nuevo León with the registration number AH17-00005. A total of 135 glenoid fossae from 135 adult Mexican individuals (i.e., ≥ 18 years-of-age), who had undergone CT scanning for non-shoulder-related reasons, were randomly selected for the purposes of this study. Coronal and axial planar images of the 135 glenoid fossae were acquired and subsequently screened for image quality and consistency in image orientation by physician clinical anatomists. Images with poor quality or inconsistent plane orientation were excluded from the study. A total of 76 coronal images and 125 axial images (65 from females and 60 from males) were ultimately included in this study, of which, 66 were included for bi-planar assessment where both coronal and axial planes were from the same patient (Table 1). Demographic information regarding age strata and sample size may be found in Table 1.

Table 1: Study population stratified by age group.

Age group (years)	CT Imaging Plane		
	Coronal	Axial	Bi-planar
>40	59	90	40
25-40	12	25	10
<25	5	10	5
Total	76 (32 ♀, 44 ♂)	125 (65 ♀, 60 ♂)	66 (26 ♀, 40 ♂)

Analysis of the contours of the glenoid fossae was accomplished via geometric morphometric methods (Zelditch *et al.*, 2004). Contours of the glenoids were delineated with TpsDig software version 2.22 (Fig. 2) (Rohlf, 2015). Contours were manually identified and then digitally resampled to be comprised of 30 equidistant semilandmarks. Landmark analysis was performed with MorphoJ software version 1.06d (Klingenberg, 2011). As part of the morphometric analysis, Procrustes superimposition, aligned by principal axes, was performed (Klingenberg, 2011; Bender-Heine *et al.*, 2017; Zdilla and Fijalkowski, 2017; Zdilla *et al.*, 2017; Zdilla *et al.*, 2018). Principal component analysis (PCA) was performed to assess whole-population variance. Whole-population variance was also demarcated according to demographic categories. Canonical variate analysis with permutation testing by MorphoJ software was performed to assess differences between sexes, ages, and sexes with respect to ages. Mahalanobis distances were calculated between demographic groups to quantify relative shape differences among the sample. Among the 66 pairs of coronal and axial images, a two-block partial least squares analysis was performed to assess the relationship between axial and coronal glenoid fossa contours.

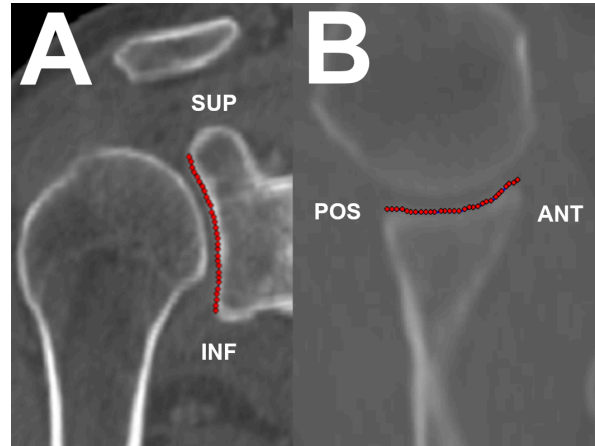


Figure 2. TpsDig software delineation of the glenoid contours. Superimposition of curves consisting of 30 equidistant landmarks in coronal (A) and axial (B) planes traversing the center of the glenoid fossa.

Results

Coronal Plane:

Principal component analysis explained 80.1% of the cumulative variance in the glenoid fossa shape with the first two principal components (PC1 = 65.7%; PC2 = 14.4%) (Fig. 3). The first principal component revealed the shape variance ranges from a pronounced concave shape to a minimally concave, nearly linear, shape (Fig. 3 and 4). The glenoid cavities varied significantly between sexes ($p < 0.0001$ from permutation tests (10,000 permutation rounds) for Mahalanobis distances among groups) (Fig. 5). Similarly, canonical variate analysis permutation tests revealed statistically significant differences among age groups (Fig. 6, Table 2). When age and sex were grouped together, CVA revealed statistically significant differences in the contours of all age/sex groupings (Fig. 7, Table 3).

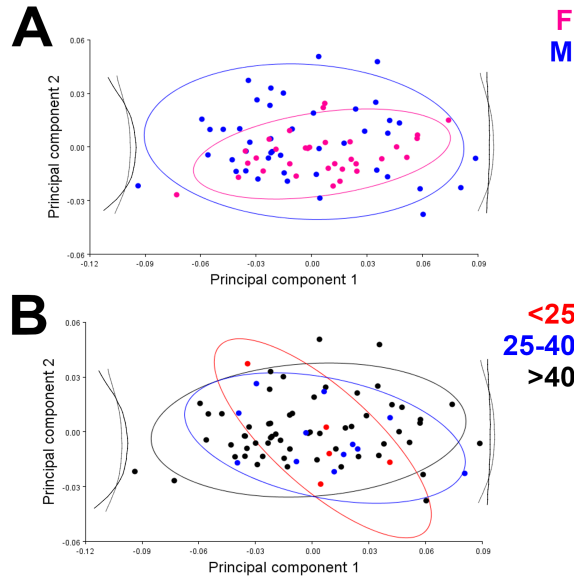


Figure 3. Principal component analysis of coronal concavity. Principal component analysis explaining 80.1% of the cumulative variance in the glenoid fossa shape with the first two principal components (PC1 = 65.7%; PC2 = 14.4%). Superimposed 95% confidence ellipses identify clustering by sexes (A) and age groupings (B).

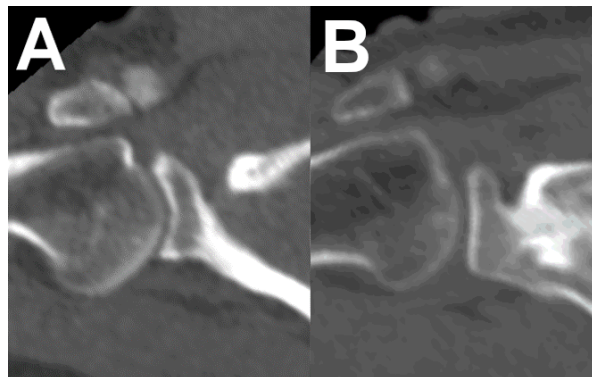


Figure 4. Coronal shoulder CT scans of glenoid fossae that represent the extreme negative and positive values of the first principal component axis corresponding to Figure 3. A: A glenoid with a particularly pronounced concavity. B: A glenoid cavity with a near absence of concavity.

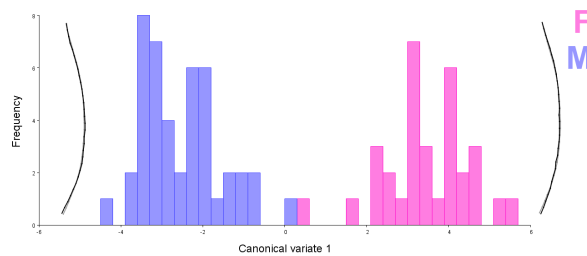


Figure 5. Canonical variate analysis comparing glenoid concavity by sex. Canonical variate analysis revealed

statistically significant differences in the glenoid contours between sexes. However, as evidenced by their average differences seen by the overlaid wireframes on the sides of the figure, minimal difference is appreciated. The most marked difference appears at the inferior lip of the glenoid represented by the contour nearest the bottom of the image, though quite subtle. The Mahalanobis distance between groups was 5.97 with a $p < 0.0001$ from permutation tests (10,000 permutation rounds) for Mahalanobis distances among groups.

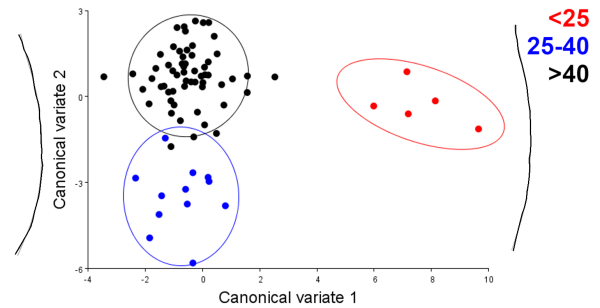


Figure 6. Canonical variate analysis comparing glenoid concavity by age group. Canonical variate analysis explaining 63.64% (CV1) and 36.36% (CV2) of variance among glenoid contours in varied age groups. All groups demonstrated a statistically significant difference in shape. The negative CV1 demonstrated a trend toward more exaggerated concavity.

Table 2: Mahalanobis distance of coronal contours of the glenoid cavity among age groups

Age (years)	<25	25-40
25-40	8.97	-
>40	$p < 0.0001$	4.23
	$p < 0.0001$	$p < 0.0001$

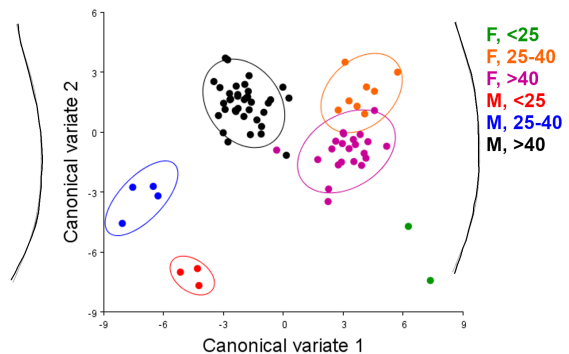


Figure 7. Canonical variate analysis comparing glenoid concavity by sex and age group. Canonical variate analysis explaining 48.25% (CV1) and 22.80% (CV2) of variance (collectively, 71.05%) among glenoid contours in varied age groups by sex. All groups demonstrated a statistically significant difference in shape. The negative CV1 denoted the most exaggerated concavity toward the inferior of the glenoid relative

to the positive CV1 axis which revealed a centrally located curve maximum.

Table 3: Mahalanobis distance of coronal contours of the glenoid cavity among sexes by age groups

Sex	Age (years)	Males			Females	
		<25	25-40	>40	<25	25-40
Males	25-40	10.36 ***	-	-	-	-
	>40	9.96 ***	9.27 ***	-	-	-
	<25	14.69 0.09	17.41 *	13.57 ***	-	-
Females	25-40	13.57 **	13.19 **	7.17 ***	11.66 *	-
	>40	11.29 ***	11.83 ***	6.16 ***	11.25 **	5.82 ***

*:p<0.05; **:p<0.005; ***:p<0.0005

Axial Plane:

Principal component analysis explained 79.46% of the cumulative variance in the glenoid fossa shape with the first two principal components (PC1 = 58.78%; PC2 = 20.68%) (Fig. 8). The first principal component revealed the shape variance to range from a pronounced concave shape to a minimally concave, nearly linear, shape (Fig. 8 and 9). The glenoid cavities varied significantly between sexes (p<0.0001 from permutation tests (10,000 permutation rounds) for Mahalanobis distances among groups) (Fig. 10). Similarly, canonical variate analysis revealed statistically significant differences among age groups (Fig. 11, Table 4). When age and sex were grouped together, CVA revealed statistically significant differences in the contours of all age/sex groupings (Fig. 12, Table 5).

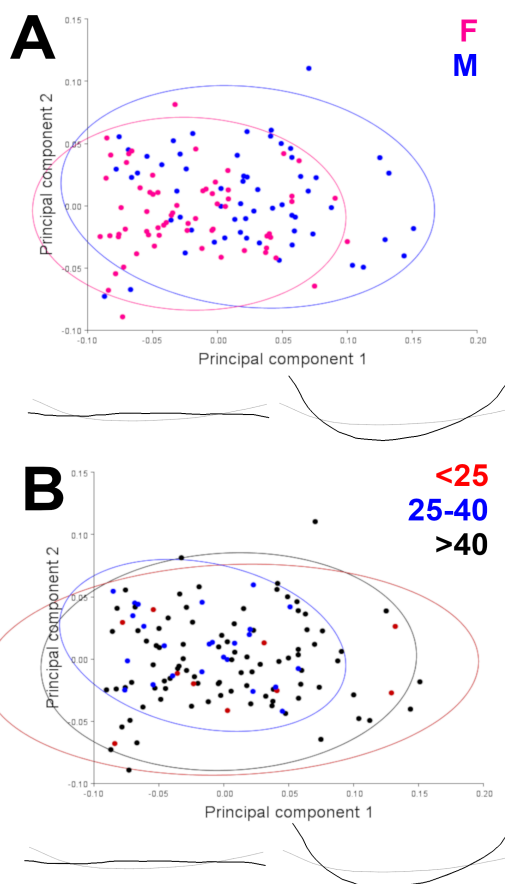


Figure 8. Principal component analysis of axial concavity. Principal component analysis explaining 79.46% of the cumulative variance in the glenoid fossa shape with the first two principal components (PC1 = 58.78%; PC2 = 20.68%). Superimposed 95% confidence ellipses identify clustering by sexes (A) and age groupings (B).

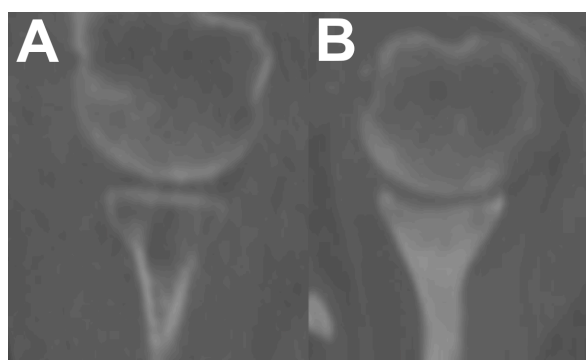


Figure 9. Axial shoulder CT scans of glenoid fossae that represent the extreme negative and positive of the first principal component axis corresponding to Figure 8. A: A glenoid cavity with a near absence of concavity. B: A glenoid with a particularly pronounced concavity.

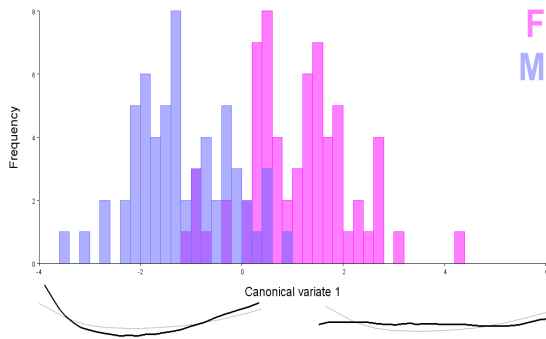


Figure 10. Canonical variate analysis comparing glenoid concavity by sex. Canonical variate analysis revealed statistically significant differences in the glenoid contours between sexes (65 females and 60 males). Males tended to have noteworthy concavity relative to females who tended to have a less-concave and more-linear appearance to the glenoid surface. The Mahalanobis distance between groups was 2.28 with a $p < 0.0001$ from permutation tests (10,000 permutation rounds) for Mahalanobis distances among groups.

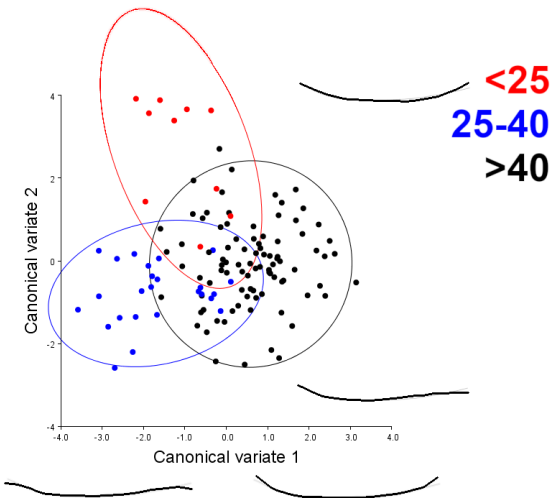


Figure 11. Canonical variate analysis comparing glenoid concavity by age group. Canonical variate explaining 57.27% (CV1) and 42.73% (CV2) of variance among glenoid contours in varied age groups. All groups demonstrated a statistically significant difference in shape. The Mahalanobis distance between 25-40 and >40-year-old groups was closer (Mahalanobis distance = 2.41) than that of <25-year-olds with the 25-40 and >40-year-old groups (Mahalanobis distance = 3.50 and 3.22, respectively). The positive CV1 demonstrated a trend toward more exaggerated concavity.

Table 4: Mahalanobis distance of axial contours of the glenoid cavity among age groups

Age (years)	<25	25-40
25-40	3.50	-
	0.0004	-
>40	3.22	2.41
	0.0001	<0.0001

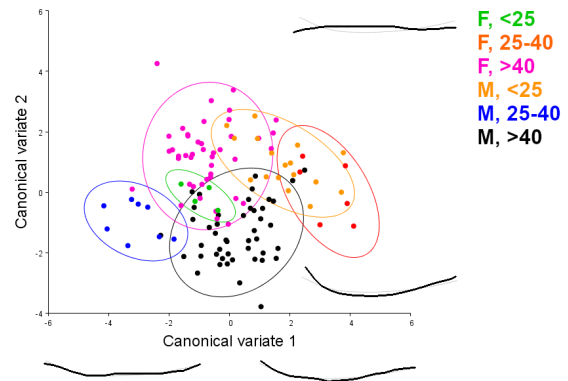


Figure 12. Canonical variate analysis comparing glenoid concavity by sex and age group. Canonical variate explaining 33.68% (CV1) and 25.50% (CV2) of variance (Collectively, 59.18%) among glenoid contours in varied age groups by sex. All groups demonstrated a statistically significant difference in shape. Female groupings clustered at the positive spectra of CV1 and CV2. Conversely, male groupings clustered at the negative spectra of CV1 and CV2. In accord with the CVA performed on sexes alone, the positive and negative aspects of CV2 represent a curvature that ranges from convex (positive CV2) to pronounced concavity (negative CV1).

Table 5: Mahalanobis distance of axial contours of the glenoid cavity among sexes by age groups

Sex	Age (years)	Males			Females	
		<25	25-40	>40	<25	25-40
Males	25-40	7.23	-	-	-	-
		***	-	-	-	-
	>40	4.55	4.35	-	-	-
		***	***	-	-	-
Females	<25	6.84	5.43	5.10	-	-
		**	*	**	-	-
	25-40	4.69	5.55	3.51	5.35	-
		***	***	***	**	-
	>40	5.00	4.31	2.75	5.11	3.57
		***	***	***	**	***

*: $p < 0.05$; **: $p < 0.005$; ***: $p < 0.0005$

Assessment of Relationship between Coronal and Axial Planes:

Two-block partial least squares analysis revealed that the axial and coronal glenoid contour shapes were dependent ($RV=0.17$, $p=0.0009$, 10,000 randomization rounds). There was 93.68% of covariation explained by PLS1 which demonstrates a significant correlation between axial and coronal contours ($r=0.44$, $p=0.0035$) (Fig. 13). Concavity in

one dimension was positively associated with concavity in the other.

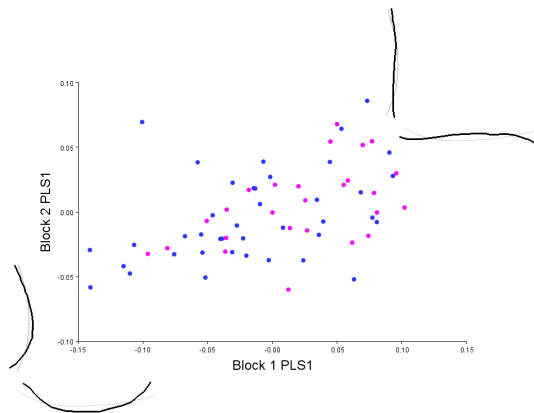


Figure 13. Two block partial least squares analysis of axial and coronal contour of the glenoid. Two block partial least squares analysis showing PLS1 that explains 93.68% of total covariation between the axial contour (Block 1) and the coronal contour (Block 2). When coronal contours are relatively concave, axial contours also tend to exhibit concavity. Conversely, when there is minimal concavity in one dimension, there tends to be minimal concavity in the other. Pink and blue data points represent female and male individuals, respectively.

Discussion

The contour of the glenoid fossa is of great clinical importance. However, the assessment of glenoid contour has been limited to classification that warrants improved interobserver reliability. This study demonstrates that geometric morphometrics can be applied as a quantifiable means of measuring the glenoid contour. This research also identified that the contours of the glenoid fossa differ between sexes, different age groups, and among sexes within varied age groups. The results of this study can be applied to improve glenohumeral joint assessment and pre-operative decision making.

Traditional morphometric measurements including height, breadth, area, and perimeter of the glenoid fossa have been utilized for determination of sexual dimorphism (Prescher and Klümpen 1995; Frutos 2002; Ozer *et al.*, 2006; Dabbs 2010; Macaluso 2011; Hudson *et al.*, 2016; Peckmann *et al.*, 2016; Peckmann *et al.*, 2017; Koukiasa *et al.*, 2017). The height and breadth of the glenoid fossa are correlated with each other (Ohl *et al.*, 2012). Males have greater glenoid height and breadth than females (Merrill *et al.*, 2012; Owaydah *et al.*, 2017). Indeed, the height and breadth of the glenoid fossa has also been

correlated with individual height and may be utilized in regression formulae for the estimation of stature (Campobasso *et al.*, 1998; Shiozono *et al.*, 2017). In addition to the structure of the glenoid fossa, males, in general, have larger scapulae relative to females (Prsecher *et al.*, 1995; Dabbs *et al.*, 2010; Papaioannou *et al.*, 2012; Peckmann *et al.*, 2016; Vassallo *et al.*, 2022; Maranhão *et al.*, 2022).

The aforementioned sexual dimorphism and allometric research provides insight for the interpretation of the data presented in this report. Since sexual dimorphism was identified in both the coronal and axial glenoid contours, it is likely that there is allometry in the glenoid, albeit not directly assessed in this report. The suggested allometry is that there is a positive relationship between glenoid size (i.e., height and breadth) and concavity, particularly in an axial plane. Future studies should assess allometry of glenoid fossa of the scapula both independent of sex and with regard to sex. Furthermore, future studies should assess the potential impact of behavior may have upon the glenoid fossa (e.g., handedness, occupation).

Regarding Walch classifications, females, having relatively small glenoids, would be more likely to have A1-type glenoids whereas males, having relatively large glenoids, are more likely to have A2-shaped glenoids based upon glenohumeral proportions.

Furthermore, the glenoid fossa has forensic value. By identifying significant differences in the shape of the glenoid fossa between sexes and age groups, this study reinforces the findings of other studies identifying forensic value in scapular size and shape (Prescher and Klümpen, 1995; Frutos, 2002; Ozer *et al.*, 2006; Merrill *et al.*, 2009; Dabbs, 2010; Macaluso, 2011; Papaioannou *et al.*, 2012; Hudson *et al.*, 2016; Peckmann *et al.*, 2016, 2017; Koukiasa *et al.*, 2017; Maranhão *et al.*, 2022; Vassallo *et al.*, 2022). The glenoid fossa of the scapula is more robust compared to other aspects of the bone that form through intramembranous ossification (e.g., inferior angle, superior angle, infraspinous fossa, supraspinous fossa). Thus, the glenoid is likely more resistant to degradation in skeletal remains. This notion is similar, to the forensic value of the relatively robust basioccipital bone (which forms via endochondral ossification) when compared to the parietal bone (which forms via intramembranous

ossification) in identifying the age-at-death from fetal cranial remains, for example (Zdilla *et al.*, 2022).

Appreciation for the variance in the shape of the glenoid fossa is also important to consider when using the glenoid fossa as a reference point from which to measure. For example, Alfaro-Gomez *et al.* (2020) recently utilized the center of the glenoid fossa to identify a coronal plane from which to identify landmarks from which to measure variation in surrounding anatomical structures including the acromion process and coracoid process of the scapula. Further, the question is raised, is a center point located half of a distance between two landmarks (e.g., superior and inferior aspect of the glenoid fossa), half the distance along a contour spanning between two landmarks (e.g., the length of the surface of the glenoid), or the point of maximum curvature of a contour (e.g., the greatest concavity of the glenoid). This report suggests that all three of these center-points could vary.

It is important to note that this study assessed glenoids among individuals who had CT performed for reasons unrelated to the glenohumeral joint and that were, otherwise, asymptomatic regarding the glenohumeral joint. On the other hand, Walch classifications are typically employed in the assessment of glenohumeral osteoarthritis. Further, the Walch classifications make little distinction between concavity and bony erosion. The most marked concavities were seen in males >40 year of age; therefore, this report may have identified bony erosion occurring in older males. However, this report identifies a greater concavity in male asymptomatic glenoids relative to female asymptomatic glenoids, regardless of age. Hence, there is a degree of independence between native bony contour and erosive change.

Varied concavity of the glenoid cavity might influence both the range of motion and the structural integrity of the glenohumeral joint. Regarding the mechanics of stability, a more concave glenoid would provide greater stability than a less-concave glenoid given the same disruptive, translational force, (traction, for example) when the humeral head is compressed against the glenoid with the same compressive force. The variance in concavity of the glenoid may be particularly important regarding inherent risk of a Bankart lesion (a fracture of the

anteroinferior glenoid labral complex) – a very common occurrence. Further, a more concave glenoid may confer additional protection against subluxation and luxation. This report identifies a positive correlation between the sagittal and axial contours. Therefore, males probably have more resistance to subluxation and luxation of the glenohumeral joint than females because of a more concave bony glenoid fossa.

Acknowledgements

This project was made possible by funding from the West Virginia Clinical and Translational Science Institute and the West Virginia University INTRO program. Research reported in this publication was supported by the National Institute of General Medical Sciences of the National Institutes of Health under Award Number 5U54GM104942-05. The content is solely the responsibility of the authors and does not necessarily represent the official views of the National Institutes of Health.

Literature Cited

- Alfaro-Gomez, U., L.D. Fuentes-Ramirez, K.I. Chavez-Blanco, J.F. Vilchez-Cavazos, M.J. Zdilla, R.E. Elizondo-Omana, J.D. Guerra-Leal, G. Elizondo-Riojas, R. Pinales-Razo, S. Guzman-Lopez, A. Quiroga-Garza. 2020. Anatomical variations of the acromial and coracoid process: clinical relevance. *Surg Radiol Anat.* **42**(8):877–885. DOI: 10.1007/s00276-020-02497-5.
- Bender-Heine, A.N., M.J. Zdilla, M.L. Russell, A.A. Rickards, J.S. Holmes, M.A. Armeni. H.W. Lambert. 2017. *Optimal costal cartilage graft selection according to cartilage shape: Anatomical considerations for rhinoplasty.* *Facial Plast Surg.* **33**(6):670-674 DOI: 10.1055/s-0037-1607972.
- Bercik, M.J., K. Kruse 2nd, M. Yalozis, M.O. Gauci, J. Chaoui, G. Walch. 2016. *A modification to the Walch classification of the glenoid in primary glenohumeral osteoarthritis using three-dimensional imaging.* *J Shoulder Elbow Surg* **25**(10):1601-1606. DOI: 10.1016/j.jse.2016.03.010.
- Bouchaib, J., P. Clavert, J.F. Kempf, J.L. Kahn. 2014. *Morphological analysis of the glenoid version in the axial plane according to age.* *Surg Radiol Anat.* **36**(6): 579-585. DOI: 10.1007/s00276-013-1238-6.
- Campobasso, C.P., G. Di Vella, F. Introna Jr. 1998. *Using scapular measurements in regression formulae for the estimation of stature.* *Boll Soc Ital Biol Sper.* **74**(7-8):75-82.
- Dabbs, G. 2010. *Sex determination using the scapula in New*

- Kingdom skeletons from Tell El-Amarna. *Homo*. **61**(6):413-420. DOI: 10.1016/j.jchb.2010.09.001.
- Denard, P.J., G. Walch. 2013. *Current concepts in the surgical management of primary glenohumeral arthritis with a biconcave glenoid*. *J Shoulder Elbow Surg*. **22**(11):1589-1598. DOI: 10.1016/j.jse.2013.06.017.
- Franklin, J.L., W.P Barrett, S.E. Jackins, F.A. Matsen 3rd. 1988. *Glenoid loosening in total shoulder arthroplasty. Association with rotator cuff deficiency*. *J Arthroplasty*. **3**(1):39-46.
- Frutos, L.R. 2002. *Determination of sex from the clavicle and scapula in a Guatemalan contemporary rural indigenous population*. *Am J Forensic Med Pathol*. **23**(3):284-288.
- Karelse, A., S. Leuridan, A. Van Tongel, P. Debeer, J. Van Der Sloten, K. Denis, L.F. De Wilde. 2015. *Consequences of reaming with flat and convex reamers for bone volume and surface area of the glenoid; a basic science study*. *Journal Orthopaedic Surgery and Research*. **10**(181). DOI: 10.1186/s13018-015-0312-7.
- Kersten, A.D., C. Flores-Hernandez, H.R. Hoenecke, D.D. D'Lima. 2015. *Posterior augmented glenoid designs preserve more bone in biconcave glenoids*. *J Shoulder Elbow Surg*. **24**(7):1135-1141. DOI: 10.1016/j.jse.2014.12.007.
- Hudson, A., T.R. Peckmann, C.J. Logar, S. Meek. 2016. *Sex determination in a contemporary Mexican population using the scapula*. *J Forensic Leg Med*. **37**:91-6. DOI: 10.1016/j.jflm.2015.11.006.
- Kidder, J.F., D.M. Rouleau, M.J. DeFranco, J. Pons-Villanueva, S. Dynamidis. 2012. *Revisited: Walch classification of the glenoid in glenohumeral osteoarthritis*. *Shoulder Elbow*. **4**:11-15.
- Klingenberg, C.P. 2011. *MorphoJ: an integrated software package for geometric morphometrics*. *Mol Ecol Resour*. **11**:353-357.
- Koukiasa, A.E., C2 Eliopoulos, S.K. Manolis. 2017. *Biometric sex estimation using the scapula and clavicle in a modern Greek population*. *Anthropol Anz*. **74**(3):241-246. DOI: 10.1127/anthranz/2017/0658.
- Lowe, J.T., E.J. Testa, X. Li, S. Miller, J.P DeAngelis, A. Jawa. 2017. *Magnetic resonance imaging is comparable to computed tomography for determination of glenoid version but does not accurately distinguish between Walch B2 and C classifications*. *J Shoulder Elbow Surg*. **26**(4):669-673. DOI: 10.1016/j.jse.2016.09.024.
- Macaluso Jr, P.J. 2011. *Sex discrimination from the glenoid cavity in black South Africans: morphometric analysis of digital photographs*. *Int J Legal Med*. **125**(6):773-778. DOI: 10.1007/s00414-010-0508-7.
- Maranho, R., M.T. Ferreira, F. Curate. 2022. *Sexual Dimorphism of the Human Scapula: A Geometric Morphometrics Study in Two Portuguese Reference Skeletal Samples*. *Forensic Sciences*. **2**(4):780-794. DOI: 10.3390/forensicsci2040056.
- Matsen 3rd, F.A., J. Clinton, J. Lynch, A. Bertelsen, M.L. Richardson. 2008. *Glenoid component failure in total shoulder arthroplasty*. *J Bone Joint Surg Am*. **90**(4):885-96. DOI: 10.2106/JBJS.G.01263.
- Merrill, A., K. Guzman, S.L. Miller. 2009. *Gender differences in glenoid anatomy: an anatomic study*. *Surg Radiol Anat*. **31**(3):183-189. DOI: 10.1007/s00276-008-0425-3.
- Nowak, D.D., T.R. Gardner, L.U. Bigliani, W.N. Levine, C.S. Ahmad. 2010. *Interobserver and intraobserver reliability of the Walch classification in primary glenohumeral arthritis*. *J Shoulder Elbow Surg*. **19**(2):180-183. DOI: 10.1016/j.jse.2009.08.003.
- Ohl, X., F. Billuar, P.Y. Lagacé, O. Gagey, N. Hagemester, W. Skalli. 2012. *3D morphometric analysis of 43 scapulae*. *Surg Radiol Anat*. **34**(5):447-453. DOI: 10.1007/s00276-012-0933-z.
- Owaydhah, W.H., M.A. Alobaidy, A.S. Alraddadi, R.W. Soames. 2017. *Three-dimensional analysis of the proximal humeral and glenoid geometry using MicroScribe 3D digitizer*. *Surg Radiol Anat*. **39**(7):767-772. DOI: 10.1007/s00276-016-1782-y.
- Ozer, I., K. Katayama, M. Sağır, E. Güleç. 2006. *Sex determination using the scapula in medieval skeletons from East Anatolia*. *Coll Antropol*. **30**(2):415-419.
- Papaioannou, V.A., E.F. Kranioti, P. Joveneaux, D. Nathena, M. Michalodimitrakis. 2012. *Sexual Dimorphism of the Scapula and the Clavicle in a Contemporary Greek Population: Applications in Forensic Identification*. *Forensic Sci Int*. **217**:231.e1-231.e7.
- Peckmann, T.R., C. Logar, S. Meek. 2016. *Sex estimation from the scapula in a contemporary Chilean population*. *Sci Justice*. **56**(5):357-363. DOI: 10.1016/j.scijus.2016.05.003.
- Peckmann, T.R., S. Scott, S. Meek, P. Mahakkanukrauh. 2017. *Sex estimation from the scapula in a contemporary Thai population: Applications for forensic anthropology*. *Sci Justice*. **57**(4):270-275. DOI: 10.1016/j.scijus.2017.02.005.
- Prescher, A., T. Klümpen. 1995. *Does the area of the glenoid cavity of the scapula show sexual dimorphism?* *J Anat*. **186**(Pt 1):223-226.
- Rohlf, F.J. TpsDig, Version 2.22, 2015. Available at: <http://life.bio.sunysb.edu/morph/>.
- Scalise, J.J., M.J. Codsì, J. Bryan, J.J. Brems, J.P. Iannotti JP. 2008. *The influence of three-dimensional computed tomography images of the shoulder in preoperative planning for total shoulder arthroplasty*. *J Bone Joint Surg Am*. **90**(11):2438-2445. DOI: 10.2106/JBJS.G.01341.
- Vassallo, S., C. Davies, L. Biehler-Gomez. 2022. *Sex Estimation Using Scapular Measurements: Discriminant Function*

- Analysis in a Modern Italian Population.* Aust J Forensic Sci. 54:785–798.
- Vo, K.V., D.J. Hackett, A.O. Gee, J.E. Hsu. 2017. *Classifications in Brief: Walch Classification of Primary Glenohumeral Osteoarthritis.* Clin Orthop Relat Res. **475**(9):2335-2340. DOI: 10.1007/s11999-017-5317-6.
- Walch, G., R. Badet, A. Boulahia, A. Khoury. 1999. *Morphologic study of the glenoid in primary glenohumeral osteoarthritis.* J Arthroplasty. **14**(6):756-760.
- Walch, G., A. Boulahia, P. Boileau, J.F. Kempf. 1998. *Primary glenohumeral osteoarthritis: clinical and radiographic classification.* The Aequalis Group. Acta Orthop Belg. **64**(Suppl 2):46-52.
- Zdilla, M.J., K.M. Fijalkowski. 2017. The Shape of the Foramen Ovale: A Visualization Aid for Cannulation Procedures. J Craniofac Surg. **28**(2):548–551. DOI: 10.1097/SCS.0000000000003325.
- Zdilla, M.J., M.L. Russell, K.N. Bliss, K.R. Mangus, A.W. Koons. 2017. *The size and shape of the foramen magnum in man.* J Craniovertebr Junction Spine. **8**(3):205-221 DOI: 10.4103/jcvjs.JCVJS_62_17.
- Zdilla, M.J., J. Skrzat, M. Kozerska, B. Leszczyński, J. Tarasiuk, S. Wroński. 2018. Oval Window Size and Shape: a Micro-CT Anatomical Study With Considerations for Stapes Surgery. Otol Neurotol. **39**(5):558–564. DOI: 10.1097/MAO.0000000000001787.
- Zdilla, M.J., J.P. Pancake, M.L. Russell, A.W. Koons. 2022. Ontogeny of the human fetal, neonatal, and infantile basioccipital bone: Traditional and extended eigenshape geometric morphometric analysis. Anat Rec. **305**(11):3230–3242. DOI: 10.1002/ar.24838.
- Zelditch, M.L., D.L. Swiderski, H.D. Sheets, and W.L. Fink. 2004. Geometric Morphometrics for biologists: a primer. Elsevier Academic Press: London. 443 pp.